



Ni supported on Mg–Al oxides for continuous catalytic wet air oxidation of Crystal Violet

Gabriel Ovejero ^{*}, Araceli Rodríguez, Ana Vallet, Juan García ^{*}

Grupo de Catálisis y Procesos de Separación (CyPS), Departamento de Ingeniería Química, Facultad de Ciencias Químicas, Universidad Complutense de Madrid, Avda. Complutense s/n, 28040 Madrid, Spain

ARTICLE INFO

Article history:

Received 11 April 2012

Received in revised form 22 May 2012

Accepted 24 May 2012

Available online 1 June 2012

Keywords:

Catalytic wet air oxidation

Crystal Violet

Nickel

Trickle-bed reactor

Wastewater

ABSTRACT

The continuous catalytic oxidation of aqueous Crystal Violet (CV) solutions has been investigated using a nickel catalysts (7 wt%) supported over Mg–Al mixed oxides in a trickle-bed reactor. The influence of the temperature, pressure, gas flow and dye initial concentration were studied in the catalytic wet air oxidation of CV. The catalyst showed a very stable activity up to 350 h on stream with an average total organic carbon (TOC) conversion of 64%. CV and TOC removal were very sensitive to the temperature. Dye conversion augmented from 44.7% at 120 °C to 86.1% at 180 °C. Dye conversion varied from 62.6 to 18.4%, TOC from 59.5 to 18.7% and TN from 66.6 to 14.0% within 10 to 50 ppm of initial dye concentration. The leaching of Ni was 6 wt% of the initial metal present in the catalyst and a 0.59% of carbonaceous deposit was formed onto the catalyst surface.

© 2012 Elsevier B.V. All rights reserved.

1. Introduction

Wet air oxidation (WAO) represents a promising technique for removal of toxic and non-biodegradable organic compounds from industrial wastewaters [1]. In this process, soluble or suspended constituents are oxidized by dissolved oxygen. The WAO process can be defined as the oxidation of organic and inorganic substances in an aqueous solution or suspension by means of oxygen or air at elevated temperatures and pressures. It has well-known capacities for breaking down biologically refractory compounds to simpler and easily treatable materials before they are released into the environment. Insoluble organic matter is converted to simpler soluble organic compounds which are in turn oxidized and eventually converted to carbon dioxide and water, without emissions of NO_x, SO₂, HCl, dioxins, furans, fly ash, etc. [1]. In general, this process takes place at high reaction temperatures (200–320 °C) and pressures (20–200 bar) by means of active oxygen species, such as hydroxyl radicals [2].

In WAO processes, the generation of active oxygen species, such as hydroxyl radicals, takes place at high temperatures and pressures. This process is known to have a great potential for the treatment of effluents containing a high content of organic matter or contaminants for which direct biological purification

is unfeasible [3]. WAO's advantages over other Advanced Oxidation Processes (AOPs) are the mentioned capacity of treatment of wastewaters with elevated chemical oxygen demand (COD) and a better cost-efficiency ratio since oxidation is an exothermic process, simple thermal balance shows that wastes with COD contents higher than approximately 20 g/l undergo autotermic wet oxidation [4,5]. The WAO process has well-known capacities for breaking down biologically refractory compounds to simpler, easily treated materials before they are released into the environment. In general, this aqueous phase flameless combustion process takes place at high reaction temperatures (473–593 K) and pressures (20–200 bar) by means of active oxygen species, such as hydroxyl radicals [2].

The use of a catalyst strongly improves the degradation of organic pollutants by using milder conditions of temperature and pressure. Soluble transition metal salts (such as iron or copper) have been reported as efficient enhancers of the reaction rate [6]. However, the recourse to a solid catalyst offers a further advantage compared with homogeneous catalysis, in principle the catalyst being easily recovered, regenerated and reused or easily set-up for continuous operation [7]. Besides, in the catalytic wet air oxidation (CWAO) process the stability and durability of the catalyst under operating condition must be strictly checked.

Co-precipitated Ni–Mg–Al hydrotalcite was found to be active for the liquid phase oxidation of alcohols and dyes [8,9], while supported iron oxide catalyst prepared from Mg–Al hydrotalcite revealed the high activity for ethylbenzene dehydrogenation [10] and for dyes treatments [11,12]. The high activities of all these

* Corresponding authors. Tel.: +34 91 394 4111; fax: +34 91 394 4114.

E-mail addresses: govejero@quim.ucm.es (G. Ovejero), juangcia@quim.ucm.es (J. García).

catalysts are undeniable due to the stable and highly dispersed active metal species [13]. In particular, Ovejero et al. [14] employed Ni supported over Mg-Al oxides for the CWAO of Crystal Violet (CV), a triarylmethane dye which is employed as a component of blue and black inks for printing, ball-pens, dyeing paper and finally as a colorant for products such as fertilizers, anti-freezes and detergents. They showed the effectiveness of this catalyst for the dye and TOC removal. Experiments of successive recycling of the catalyst were performed showing no leaching of the metal and no remarkable loss of its activity. However, as it was stated by the authors, continuous experiments in trickle-bed reactor must be performed to confirm the stability of the catalyst for a possible industrial application.

In this work, we aimed at the preparation of nickel catalysts supported over Mg-Al mixed oxides by incipient wetness impregnation technique for the CWAO of CV in a trickle-bed reactor to study the catalyst stability and the process efficiency. The effect of operational conditions such as temperature, pressure, gas flow and initial dye concentration will be also tested.

2. Experimental

2.1. Materials and synthesis of catalysts

CV was selected as the model pollutant because it is hardly biodegradable by the conventional biological processes, but widely employed in the textile, colour solvent, ink, paint, paper, pharmaceutical and plastic industries. The dye was purchased from Sigma-Aldrich (Steinheim, Germany) and used without further purification. The main characteristics and properties of this dye and its structure can be consulted elsewhere [14].

2.2. Preparation of the catalyst

HT precursor was employed as support in the preparation of nickel catalysts. It was prepared by the co-precipitation method proposed by Yamaguchi et al. [15]. $\text{Mg}(\text{NO}_3)_2 \cdot 6\text{H}_2\text{O}$ and $\text{Al}(\text{NO}_3)_2 \cdot 9\text{H}_2\text{O}$ (Sigma-Aldrich, Steinheim, Germany) in desired amounts were dissolved in 600 ml of water to form solution A. Besides, Na_2CO_3 and NaOH were mixed in 300 ml of water to form solution B. Solution B was stirred for 1 h at constant temperature of 65 °C. Then, solution A was slowly dropped forming a precipitate [16]. The resulting solution was aged at 60 °C for 18 h. Then, it was filtered and washed with distilled water at 40 °C for 2 h. The resulting precipitates were dried at 100 °C for 12 h.

Nickel catalyst was prepared by incipient wetness impregnation technique employing $\text{Ni}(\text{NO}_3)_2 \cdot 6\text{H}_2\text{O}$ purchased from Panreac (Barcelona, Spain) in aqueous solution as precursor. The precursor amount was calculated to obtain a catalyst load of 7 wt% of nickel in the final analysis. $\text{Ni}(\text{NO}_3)_2 \cdot 6\text{H}_2\text{O}$ solution was added onto the fresh hydrotalcite, and the resulting solid was calcined at 550 °C for 5 h.

2.3. Characterization

The support and the nickel catalyst were characterized by physical adsorption of nitrogen at –196 °C in a Micromeritics ASAP 2010 apparatus. XRD patterns were recorded using a SIEMENS D-501 diffractometer. The metal loading was determined by mean of X-Ray Fluorescence (XRF) (Broker S4 Explorer). More detailed characterization procedures can be found in previous work [14].

2.4. CWAO reactions

Continuous experiments were carried out in a Microactivity-Reference unit (PID Eng&Tech, model MA-Ref), which is an automated and computer-controlled continuous-flow trickle-bed

laboratory reactor. Concentrations of the fed aqueous solutions ranged from 25 to 100 ppm. A fixed-bed tubular reactor in Hastelloy C-276 was heated with a reactor furnace and integrated within the hot box system, which includes an electric forced convection heater which permits the process route to be preheated and kept at temperatures up to 190 °C. The liquid reactant was introduced into the unit using a HPLC positive alternative displacement pump (Gilson, model 307). The oxygen source in these experiments was air, which was fed to the system through an electronic mass-flow controller. The preheated gas and liquid streams merge in a T-joint and are then introduced to the top of the reactor through a 10 mm sintered 316 stainless-steel filter (another is located at the outlet of the reactor, which protected the arrangement from possible catalyst fines). A porous (2 mm) plate made of Hastelloy C-276, supported on a 316 stainless-steel pipe, was placed inside and near the middle of the reactor tube to support the fixed bed composed of 1.4 g of Ni/MgAlO catalyst placed over inert spherical glass beads. The reaction temperature was measured by a thermocouple, which was inserted through the upper end of reactor and was in contact with the catalyst bed. The thermocouple was regulated from the pre-set temperature by a PID temperature controller (TOHO, model TTM-005). The gas and liquid phases, which passed the catalytic bed in a co-current downflow mode and flowed out at the bottom of the reactor, were separated in a high-pressure liquid-gas (L/G) separator cooled with a Peltier cell. The L/G separator equipped with a micrometric servo-controlled valve and capacitive level sensor provides an efficient liquid discharge from the unit [13].

The temperature (from 120 to 180 °C), initial dye concentration (from 25 to 100 ppm), air pressure (from 25 to 60 bar), effluent flow (from 0.1 to 0.7 mL min^{-1}), and air flow (from 100 to 300 mL min^{-1} , which was in excess with respect to the stoichiometry for total oxidation) were set at each experiment at the desired values. The effluent at the outlet was periodically collected and analyzed.

2.5. Procedures and analysis

CV concentration was determined by the reduction of absorbance of the wavelength corresponding to its maximum UV-vis absorption ($\lambda_{\text{CV}} = 588 \text{ nm}$) using an UV-vis Shimadzu spectrophotometer. Total Organic Carbon (TOC) and Total Nitrogen (TN) measurements were carried out on a Shimadzu TOC analyzer coupled with a TN unit (TNM-1), to evaluate the extent of mineralization of the dye. Ammonium, nitrite and nitrate ions were analyzed after dilution using ion selective electrodes (ISE). Crison NO_3^- 9662; Crison NO_2^- 9664 and Crison NH_4^+ 9663 electrodes were used in the pH meter (Crison model pH Meter Basic 20) to determine the amounts of the cited ions in the effluents. All solutions were stirred with a magnetic stirrer. Final effluents were analyzed by ICP-AES in order to evaluate the leaching of active species to the liquid phase.

HPLC analyses were performed in a Varian Prostar-230 apparatus with a C18. The flow rate of the mobile phase was set at 1.0 mL min^{-1} . Solvent A was 25 mM aqueous ammonium acetate buffer (pH 6.9), while solvent B was methanol. A linear gradient was set as follows: $t=0, C=95$; $t=20, C=50$; $t=45, C=10$; $t=50, C=95$.

3. Results and discussion

3.1. Catalyst characterization

Detailed results for the solid characterization can be consulted in previous publications [14]. It was proved that in the presence of nickel, the BET area of the solid decreased from 182 to 169 $\text{m}^2 \text{g}^{-1}$. It

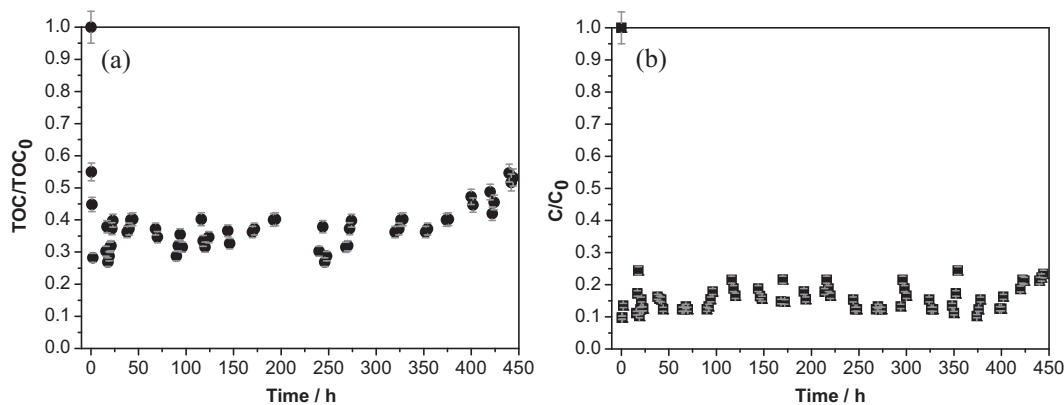


Fig. 1. (a) CV and (b) TOC degradation in long-term reaction at 180 °C, 50 bar, 0.5 mL min⁻¹ ($T_R = 0.19 \text{ g}_{\text{Ni}} \text{ min mL}^{-1}$) and 25 ppm.

was also shown that the metallic particles exhibited a high metallic dispersion (27%). No remarkable differences in the XRD patterns were found for the uncalled catalyst and the support, indicating that the inclusion of the Ni cation by wetness impregnation did not affect the HT structure. After calcination at 550 °C the formation of mixed oxides structures of Mg and Al was observed [14].

3.2. Experiments in trickle-bed reactor

3.2.1. Catalyst stability

To prove the catalyst stability a long-term reaction (450 h) was carried out in the trickle-bed reactor. The efficiency of the oxidation of CV aqueous solution was tested in terms of two usually adopted indicators for global degradation performance: colour bleaching by removal of the most intense absorption peak at 588 nm and TOC removal [17]. Fig. 1a shows the normalized changes in TOC and CV concentration as a function of time on stream in oxidation runs, carried out with an initial dye concentration of 25 ppm at 0.5 mL min⁻¹ ($T_R = 0.19 \text{ g}_{\text{Ni}} \text{ min mL}^{-1}$) flow rates, 180 °C and 50 bar in the presence of Ni/MgAlO. After starting flowing the dye solution, TOC concentration decreased rapidly during the first 6 h. After this transition period, TOC concentration reached a steady state regime for this given experimental conditions. The catalyst showed a very stable activity up to 350 h on stream with an average TOC conversion of 64%. After the first 350 h, TOC conversion clearly decreased to a final value 45% at 450 h. There is a clear loss of the catalyst activity after this point.

This loss of catalytic activity is not due to the leaching of a 6 wt% of the initial nickel present in the catalyst, as this phenomenon occurs only within the 4 first hours of the reaction. Besides, a 0.59% of carbonaceous deposit is formed onto the catalyst surface but no remarkable differences in the surface area are observed after the reaction (from 143.2 to 137.3 m² g⁻¹). The variation in TOC conversion might then be due to these carbonaceous substances which make more difficult the access of the dissolved compounds to the active sites, causing a decrease in TOC conversion [18].

On the other hand, no decay in the dye conversion was observed in Fig. 1b. After 350 h, the catalyst might be active to destroy the CV molecules but not enough to degrade the most recalcitrant reaction products. These experiments show that despite the formation of carbonaceous compounds onto the catalyst surface, it presents a good stability in the considered reaction conditions.

3.2.2. Effect of the temperature

Results in Fig. 2 showed that CV and TOC removal were very sensitive to the temperature. Dye conversion augmented from 44.7% at 120 °C to 86.1% at 180 °C. Little difference was observed between

the reactions carried out at 120 and 150 °C when TOC removal is considered (56.8 and 59.4%, respectively) while a conversion of 69.4% is reached at 180 °C. The same tendencies were observed when the reaction was carried out in the batch reactor. The causes of this evolution with the temperature have already been explained by Ovejero et al. [14]. In addition, no remarkable differences with the temperature were observed when considering the TN removal. For the reaction carried out at 120 and 150 °C the distribution of the N-containing by-products was similar and led mainly to the formation of ammonia whereas at 180 °C the formation of undesirable nitrates and nitrites was dominant. This is in accordance with the findings of Barbier et al. [19] for the oxidation of aniline with a Ru/CeO₂ catalyst.

Residence times were varied in the range 0.14–0.98 g_{Ni} min mL⁻¹ (from 0.7 to 0.1 mL min⁻¹) at each temperature to check the influence of this variable. For CV, TOC and TN removal the influence of the liquid flow rate was higher for the lower temperatures. As expected, a decrease in liquid flow rate (i.e. an increase in the space time) gave higher CV, TOC and TN conversion (Fig. 3a–c). However, when the liquid flow was set at 0.1 mL min⁻¹ ($T_R = 0.98 \text{ g}_{\text{Ni}} \text{ min mL}^{-1}$) no significant improvements were shown in TOC and CV removal compared to 0.2 mL min⁻¹ ($T_R = 0.49 \text{ g}_{\text{Ni}} \text{ min mL}^{-1}$). This might be due to an insufficient wetting of the catalyst and incomplete catalyst utilization [20]. Another reason might be that a maximum of mineralization has been attained for this temperature due to the presence of refractory intermediate compounds such as acetic acid

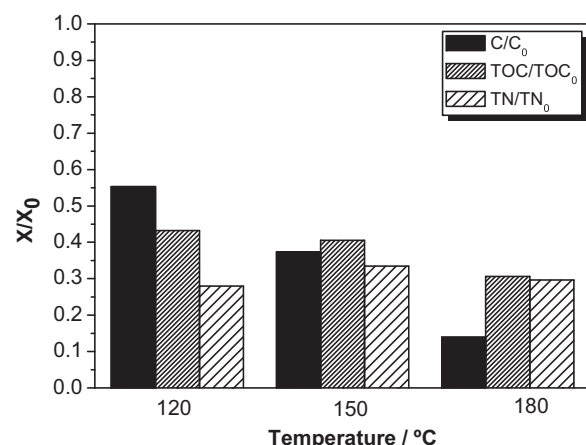


Fig. 2. CV, TOC and TN conversion with the temperature at 50 bar, 25 ppm, 0.5 mL min⁻¹ ($T_R = 0.19 \text{ g}_{\text{Ni}} \text{ min mL}^{-1}$).

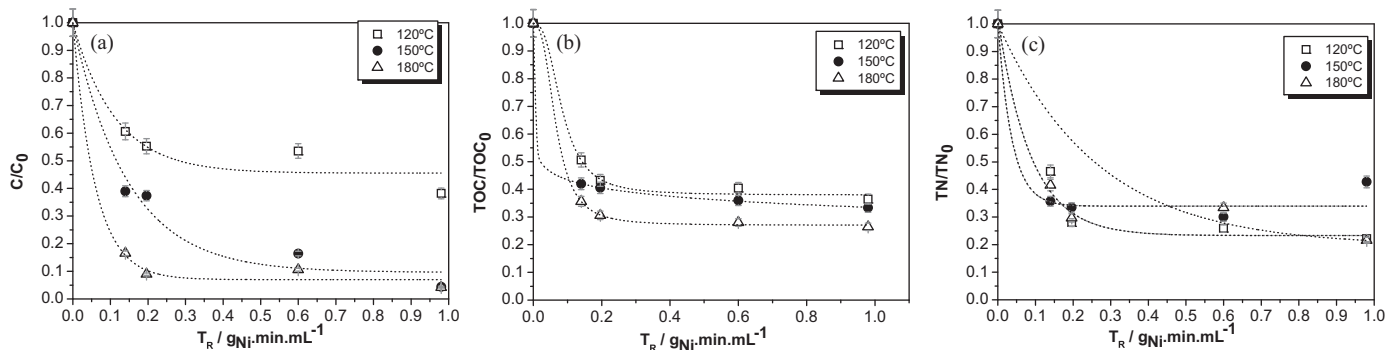


Fig. 3. (a) CV, (b) TOC and (c) TN removal as a function of T_R at different temperatures at 50 bar, 25 ppm.

formic acids which were detected by HPLC analyses. More details about reaction intermediates will be given on further publications.

To find out if there is incomplete catalyst utilization we proceeded as following. The solutions collected at the outlet of the reactor during the preceding steady state operations were each recycled through the catalyst bed, using the same reaction conditions, thus the same hydrodynamic conditions. This results in a double space time for the initial solution. No improvements in CV or TOC removal for a given space time were observed using this methodology (not shown). Therefore, one can conclude that there is no wetting inefficiency during the process at this liquid flow and the maximal CV and TOC conversion possible at this temperature has already been reached. For example, at 180 °C and $T_R = 0.98 \text{ g}_{Ni} \text{ min mL}^{-1}$ the conversion of CV was almost complete (98%), but increasing amounts of acetic and formic acid, detected by HPLC, were observed in comparison with the reactions carried out at lower temperatures. As a consequence, TOC abatement improves slowly with the temperature towards an asymptotic value compared with dye conversion. The difference observed between CV and dye removal corresponds to an accumulation of reaction intermediates in the aqueous phase. Furthermore, the intermediate products detected in the trickle-bed reactor operation were the same as in the batch experiments [14]. Thus, we can expect the same reaction mechanism in both reactors.

Table 1 shows a comparison of the initial activities in the batch and trickle bed reactor (at 0.5 ml min^{-1} or $T_R = 0.98 \text{ g}_{Ni} \text{ min mL}^{-1}$) under the same reaction conditions (pressure and initial concentration). It can be observed that the initial activity is higher in the batch reactor, especially at higher temperatures. This could be due to the fact that the reaction in the trickle-bed reactor needs a certain time to reach the steady state. This operational delay may lead to lower initial activities.

Since TOC analysis provides only information about the removal of total organic carbon from the liquid-phase, selectivity towards non-organic compounds (S_{NOC}) was defined as $100 (X_{TOC}/X_{dye})$ where X_{TOC} and X_{dye} are TOC and dye conversion, respectively.

Calculated S_{NOC} for the reaction at 0.5 ml min^{-1} at temperatures between 120 and 180 °C had values above 76.2% reaching a 98% at the lowest temperature. These values are similar to those obtained in the batch reactor, which ranged from 55.3 to 98.6% for the same initial dye concentration, temperatures and pressure [14].

Table 1
Comparison of the initial activities in batch and trickle-bed reactor.

	Initial activity ($\text{mmol min}^{-1} \text{g}_{Ni}^{-1}$)		
	120 °C	150 °C	180 °C
Batch	7.4×10^{-3}	1.1×10^{-3}	8.51×10^{-4}
Trickle-bed	7.7×10^{-3}	1.2×10^{-4}	1.2×10^{-4}

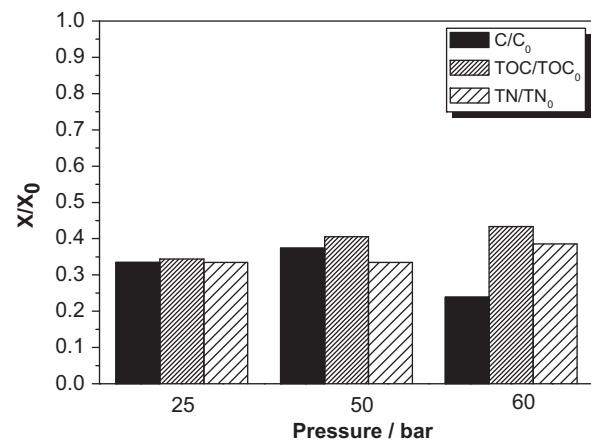


Fig. 4. CV, TOC and TN conversion with the pressure at 150 °C, 25 ppm, 0.5 mL min^{-1} .

3.2.3. Effect of the pressure

As shown in Fig. 4, the conversion of CV improved when the total pressure increased. This effect was only noticeable when the total pressure increased from 50 to 60 bar, while the difference between 25 and 50 bar was somewhat insignificant. On the other hand, TOC removal decreased with pressure. At 25 bar TOC conversion attained the 65.6% while at 60 bar this value was only 56%. This might suggest that an increase in the total pressure is responsible for the catalyst deactivation. ICP analysis showed no differences in the nickel leachates with the reaction pressure and the values were similar to those indicated in Section 3.2.1. Individual reactions at each pressure were carried out to perform detailed analysis of the employed catalysts. BET analysis showed no remarkable differences on the catalyst surface areas (from 162 to $155 \text{ m}^2 \text{ g}^{-1}$), as shown in Table 2. However, TOC analysis of the catalyst after reaction revealed the presence of adsorbed products, possibly polymeric compounds, on the catalyst surface which augmented with total pressure (from 0.05 to 0.59 wt% C). These

Table 2
Catalyst surface areas and percentages of carbonaceous deposition after reaction at each pressure.

	BET area ($\text{m}^2 \text{ g}^{-1}$)	C (wt%)
Fresh catalyst	162	0.05
25 bar	160	0.33
50 bar	155	0.36
60 bar	156	0.59

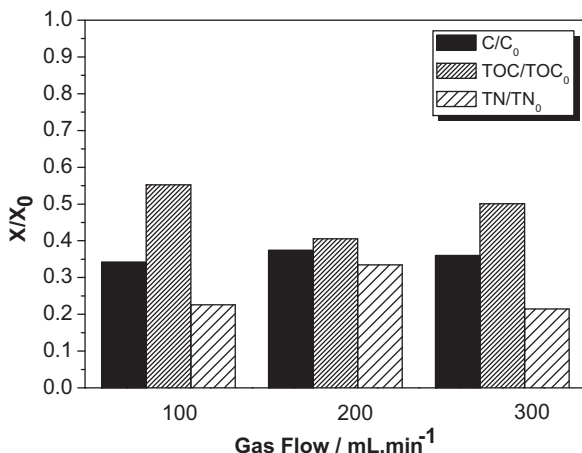


Fig. 5. CV, TOC and TN conversion with the gas flow at 150 °C, 25 ppm, 0.5 mL min⁻¹.

carbonaceous substances could make more difficult the access of the dissolved compounds to the active sites, causing a decrease in TOC conversion. As far as TN is concerned, the pressure variation does not affect to the nitrogen degradation.

3.2.4. Effect of the gas flow

Given the employed experimental conditions, all oxidation runs performed in this study were conducted in a low-interaction trickle-flow regime, which means that the liquid trickles down the packing in the form of droplets, films and rivulets, while the continuous gas phase occupies the remaining porous space and flows separately [21].

Fig. 5 shows that gas flow has any effect in the dye conversion, as this value is close to 64% for each employed gas flow. However, TOC removal presents a maximal conversion at 200 mL min⁻¹.

A palpable explanation for this observation is related to the higher gas superficial velocities, so the gas phase has a more prominent effect on the agglomeration of liquid within the catalytic bed, producing less liquid holdup. The higher gas superficial velocities resulted in lower liquid holdup as one would expect under steady-state operation [22]. This fact could explain the decrease of TOC conversion above 200 mL min⁻¹.

On the other hand, at high pressure, the gas flow reduces the liquid hold-up considerably, due to the increase of the drag force in the liquid-gas interface, explaining the observed enhancement of TOC conversion from 100 to 200 mL min⁻¹ [23]. Also, if TN removal is considered, a minimal in conversion is found at the same flow rate.

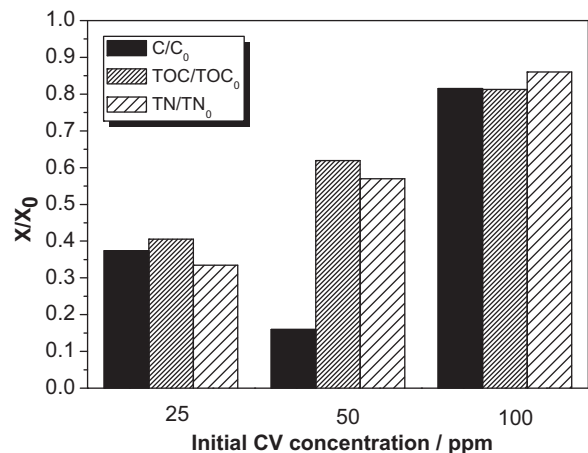


Fig. 6. CV, TOC and TN conversion with the initial CV concentration at 150 °C, 25 ppm, 0.5 mL min⁻¹.

3.2.5. Effect of the dye concentration

Fig. 6 shows the effect of the initial dye concentration on CV, TOC and TN removal. It can be clearly seen that when the initial concentration increased, the conversion decreased dramatically. This is in contrast with the obtained results in batch reactor [14] where no difference in final conversion was observed while modifying the initial CV concentration from 25 to 100 ppm.

As an example, dye conversion varied from 62.6 to 18.4%, TOC from 59.5 to 18.7% and TN from 66.6 to 14.0% within 10 to 50 ppm. This phenomenon may be attributed to the fact that, with an increase in the initial dye concentration and the dose of catalyst kept constant; more dye molecules are absorbed onto the surface of the catalyst. Thus, the number of substrates accommodated in the lattice of the catalyst increases and inhibits the action of the catalyst with oxygen molecules, thereby decreasing the degradation efficiency.

It is worth noticing that at 100 ppm the TOC and CV conversion are similar meaning that the selectivity towards non-organic compounds is near the 100%.

Fig. 7 shows the effect of residence time at different initial dye concentrations. As observed for the experiments at different temperatures (Fig. 3), higher residence times gave better results in TOC conversion. For CV and TN conversion, above 0.6 g_{Ni} min mL⁻¹ no improvements are made when increasing the residence time. As explained in Section 3.2.1 this could be due to the formation of refractory reaction intermediates that cannot be oxidized with the employed reaction conditions.

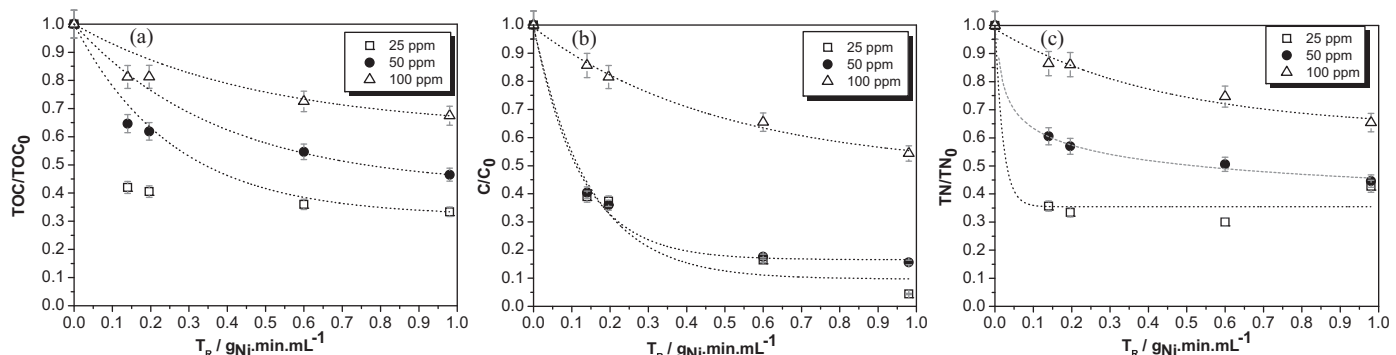


Fig. 7. (a) CV, (b) TOC and (c) TN removal as a function of T_R at different initial CV concentration at 150 °C, 25 ppm.

4. Conclusions

The oxidation of aqueous Cristal Violet was conducted in mild conditions of temperature (120–180 °C), total pressure (25–60 bar) and residence time (0.14 to 0.98 g_{Ni} min mL⁻¹) in a trickle-bed reactor. Ni catalyst (7 wt%) supported over Mg-Al mixed oxides was demonstrated to have a positive catalytic effect on the wet oxidation of this dye. After the first 350 h reaction time (average TOC conversion of 64%), TOC conversion clearly decreased to a final value 45% at 450 h. There is a clear loss of the catalyst activity after this point. Dye conversion varied from 62.6 to 18.4%, TOC from 59.5 to 18.7% and TN from 66.6 to 14.0% within 10 to 50 ppm. For CV, TOC and TN removal the influence of the liquid flow rate was higher for the lower temperatures. Calculated S_{NOC} for the reaction at 0.5 ml min⁻¹ at temperatures between 120 and 180 °C had values above 76.2% reaching a 98% at the lowest temperature.

Acknowledgements

The authors gratefully acknowledge the financial support from Ministerio de Economía y Competitividad CTQ2011-27169, by CONSOLIDER Program through TRAGUA Network CSD2006-44, and Comunidad de Madrid through REMTAVARES Network S2009/AMB-1588.

References

- [1] F. Luck, *Catalysis Today* 53 (1999) 81.
- [2] J. Levec, A. Pintar, *Catalysis Today* 124 (2007) 172–184.
- [3] V.S. Mishra, V.V. Mahajani, J.B. Joshi, *Industrial and Engineering Chemistry Research* 34 (1995) 2–48.
- [4] R. Andreozzi, V. Caprio, A. Insola, R. Marotta, *Catalysis Today* 53 (1999) 51–59.
- [5] S. Esplugas, J. Giménez, S. Contreras, S. Pascual, M. Rodríguez, *Water Research* 36 (2002) 1034–1042.
- [6] D. Mantzavinos, R. Hellenbrand, A.G. Livingston, I.S. Metcalfe, *Applied Catalysis B-Environmental* 7 (1996) 379–396.
- [7] K.-H. Kim, S.-K. Ihm, *Journal of Hazardous Materials* 186 (2011) 16–34.
- [8] T. Kawabata, Y. Shinozuka, Y. Ohishi, T. Shishido, K. Takaki, K. Takehira, *Journal of Molecular Catalysis A-Chemical* 236 (2005) 206–215.
- [9] A. Vallet, G. Ovejero, A. Rodríguez, J. García, *Chemical and Engineering Transactions* 24 (2011) 1273–1278.
- [10] Y. Ohishi, T. Kawabata, T. Shishido, K. Takaki, Q. Zhang, Y. Wang, K. Nomura, K. Takehira, *Applied Catalysis A-General* 288 (2005) 220–231.
- [11] G. Ovejero, A. Rodríguez, A. Vallet, P. Gómez, J. García, *Water Science and Technology* 63 (2011) 2381–2387.
- [12] G. Ovejero, A. Rodríguez, A. Vallet, J. García, *Environmental Science and Pollution Research* 18 (2011) 1518–1526.
- [13] M. Shiraga, T. Kawabata, D. Li, T. Shishido, K. Komaguchi, T. Sano, K. Takehira, *Applied Clay Science* 33 (2006) 247–259.
- [14] G. Ovejero, A. Rodríguez, A. Vallet, S. Willerich, J. García, *Applied Catalysis B-Environmental* 111–112 (2011) 586–594.
- [15] K. Yamaguchi, K. Ebitani, K. Kaneda, *Journal of Organic Chemistry* 64 (1999) 2966–2968.
- [16] F. Basile, P. Benito, G. Fornasari, A. Vaccari, *Applied Clay Science* 48 (2010) 250–259.
- [17] C. Diaz-Taboada, J. Batista, A. Pintar, J. Levec, *Applied Catalysis B-Environmental* 89 (2009) 375–382.
- [18] M. Besson, P. Gallezot, *Catalysis Today* 81 (2003) 547–559.
- [19] J. Barbier, L. Oliviero, B. Renard, D. Duprez, *Catalysis Today* 75 (2002) 29–34.
- [20] V. Tukac, J. Hanika, *Journal of Chemical Technology and Biotechnology* 71 (1998) 262–266.
- [21] Q. Wu, X. Hu, P.-L. Yue, J. Feng, X. Chen, H. Zhang, S. Qiao, *Separation and Purification Technology* 67 (2009) 158–165.
- [22] R.J.G. Lopes, V.S.L. de Sousa, R.M. Quinta-Ferreira, *Chemical Engineering Science* 66 (2011) 3280–3290.
- [23] F. Pironti, D. Mizrahi, A. Acosta, D. González-Mendizabal, *Chemical Engineering Science* 54 (1999) 3793–3800.